Insulin Internalizes GLUT2 in the Enterocytes of Healthy but Not Insulin-Resistant Mice

Vanessa Tobin,[1,2,3] Maude Le Gall,[1,2,3] Xavier Fioramonti,[4] Emilie Stolarczyk,[1,2,3] Alba G. Blazquez,[5] Christophe Klein,[6] Magali Prigent,[7] Patricia Serradas,[1,2,3] Marie-Hélène Cuif,[7] Christophe Magnan,[4] Armelle Leturque,[1,2,3] and Edith Brot-Laroche[1,2,3]

OBJECTIVES—A physiological adaptation to a sugar-rich meal is achieved by increased sugar uptake to match dietary load, resulting from a rapid transient translocation of the fructose/glucose GLUT2 transporter to the brush border membrane (BBM) of enterocytes. The aim of this study was to define the contributors and physiological mechanisms controlling intestinal sugar absorption, focusing on the action of insulin and the contribution of GLUT2-mediated transport.

RESEARCH DESIGN AND METHODS—The studies were performed in the human enterocytic colon carcinoma TC7 subclone (Caco-2/TC7) cells and in vivo during hyperinsulinemic-euglycemic clamp experiments in conscious mice. Chronic high-fructose or high-fat diets were used to induce glucose intolerance and insulin resistance in mice.

RESULTS AND CONCLUSIONS—In Caco-2/TC7 cells, insulin action diminished the transepithelial transfer of sugar and reduced BBM and basolateral membrane (BLM) GLUT2 levels, demonstrating that insulin can target sugar absorption by controlling the membrane localization of GLUT2 in enterocytes. Similarly, in hyperinsulinemic-euglycemic clamp experiments in sensitive mice, insulin abolished GLUT2 (i.e., the cytochalasin B-sensitive component of fructose absorption), decreased BBM GLUT2, and concomitantly increased intracellular GLUT2. Acute insulin treatment before sugar intake prevented the insertion of GLUT2 into the BBM. Insulin resistance in mice provoked a loss of GLUT2 trafficking, and GLUT2 levels remained permanently high in the BBM and low in the BLM. We propose that, in addition to its peripheral effects, insulin inhibits intestinal sugar absorption to prevent excessive blood glucose excursion after a sugar meal. This protective mechanism is lost in the insulin-resistant state induced by high-fat or high-fructose feeding. ***Diabetes* 57: 555–562, 2008**

From the [1]Université Pierre et Marie Curie-Paris 6, Unité Mixte de Recherche S 872, Paris, France; [2]Institut National de la Santé et de la Recherche Médicale, Unité Mixte de Recherche S 872, Paris, France; [3]Université Paris Descartes-Paris 5, Unité Mixte de Recherche S 872, Paris, France; [4]Université Paris 7, Centre National de la Recherche Scientifique, Paris, France; [5]Laboratory of Experimental Pathology and Drug Targeting, University of Salamanca, CIBERehd, Spain; [6]IFR58, Centre de Recherche des Cordeliers, Paris, France; [7]Institut de Génétique et Microbiologie, Centre Scientifique d'Orsay, Université Paris 11-Orsay, Orsay, France.

Address correspondence and reprint requests to Edith Brot-Laroche, CRC, Team 9, 15 rue de l'Ecole de Médecine, 75006 Paris, France. E-mail: edith.brot-laroche@crc.jussieu.fr.

Received for publication 16 July 2007 and accepted in revised form 20 November 2007.

Published ahead of print at http://diabetes.diabetesjournals.org on 5 December 2007. DOI: 10.2337/db07-0928.

Additional information for this article can be found in an online appendix at http://dx.doi.org/10.2337/db07-0928.

BBM, brush border membrane; BLM, basolateral membrane; Caco-2/TC7, colon carcinoma TC7 subclone; GIR, glucose infusion rate; 3-OMG, [^{3}H]-3-*O*-methyl-glucose; PepT1, peptide transporter-1; PiP_3, phosphatidylinositol (3,4,5)-trisphosphate; SGLT1, sodium-dependent glucose cotransporter.

Intestinal sugar transport constantly adapts to the dietary environment. At low levels, the end products of carbohydrate digestion are absorbed by a two-step membrane-transport process involving the sodium-dependent glucose cotransporter (SGLT1) and the facilitative fructose transporter (GLUT5) in the brush border membrane (BBM) (1) lining the lumen. GLUT2 in the basolateral membrane (BLM) (2) ensures sugar exit into the blood stream (3). The level of sugar absorption is also regulated by a rapid and transient recruitment of GLUT2 into enterocyte BBM (4,5). A high sugar intake is a physiological regulator of this process, increasing monosaccharide uptake threefold in vivo (6). The recruitment of GLUT2 in BBM was also observed in conditions of increased calorie demand and glucagon-like peptide 2 treatment (7–11).

The mechanisms by which GLUT2 leaves the BBM in the absence of luminal sugar (interprandial periods) are unknown. Of the possible physiological stimuli occurring during feeding, insulin was thought to be a candidate because it exerts systemic hypoglycemic effects by stimulating the translocation of GLUT4 into the plasma membrane of skeletal muscle and adipose cells (rev. in 12) and decreasing liver glucose output. Furthermore, the presence of GLUT2 in BBM was initially found under conditions of experimental diabetes, i.e., lack of insulin and consequent hyperglycemia (13). The underlying mechanisms for the loss of BBM GLUT2, i.e., degradation, internalization, and transcytosis, need to be determined.

An acute inhibition of sugar absorption by insulin was interpreted as being an indirect consequence of metabolic flow and entirely attributed to SGLT1 (14). The aim of this study was therefore to analyze the impact of insulin on intestinal sugar absorption, focusing on the localization of GLUT2 in enterocyte membranes in colon carcinoma TC7 subclone (Caco-2/TC7) cells (15) and in vivo in mice. In addition, we aimed to establish whether enterocytes would respond to elevated blood glucose or to plasma insulin under hyperinsulinemic-euglycemic clamp conditions or during the course of a test meal in mice. An increased consumption of fructose is suspected of triggering metabolic disorders including glucose intolerance and insulin resistance (16,17). Glucose homeostasis disorders are also obtained with prolonged exposure to a high-fat diet. A comparison was therefore made of normal and insulin-resistant states using chronic high-fructose or high-fat dieting and associate metabolic disturbances as tools to provide insight into the control by insulin of GLUT2 membrane localization in intestinal membranes.

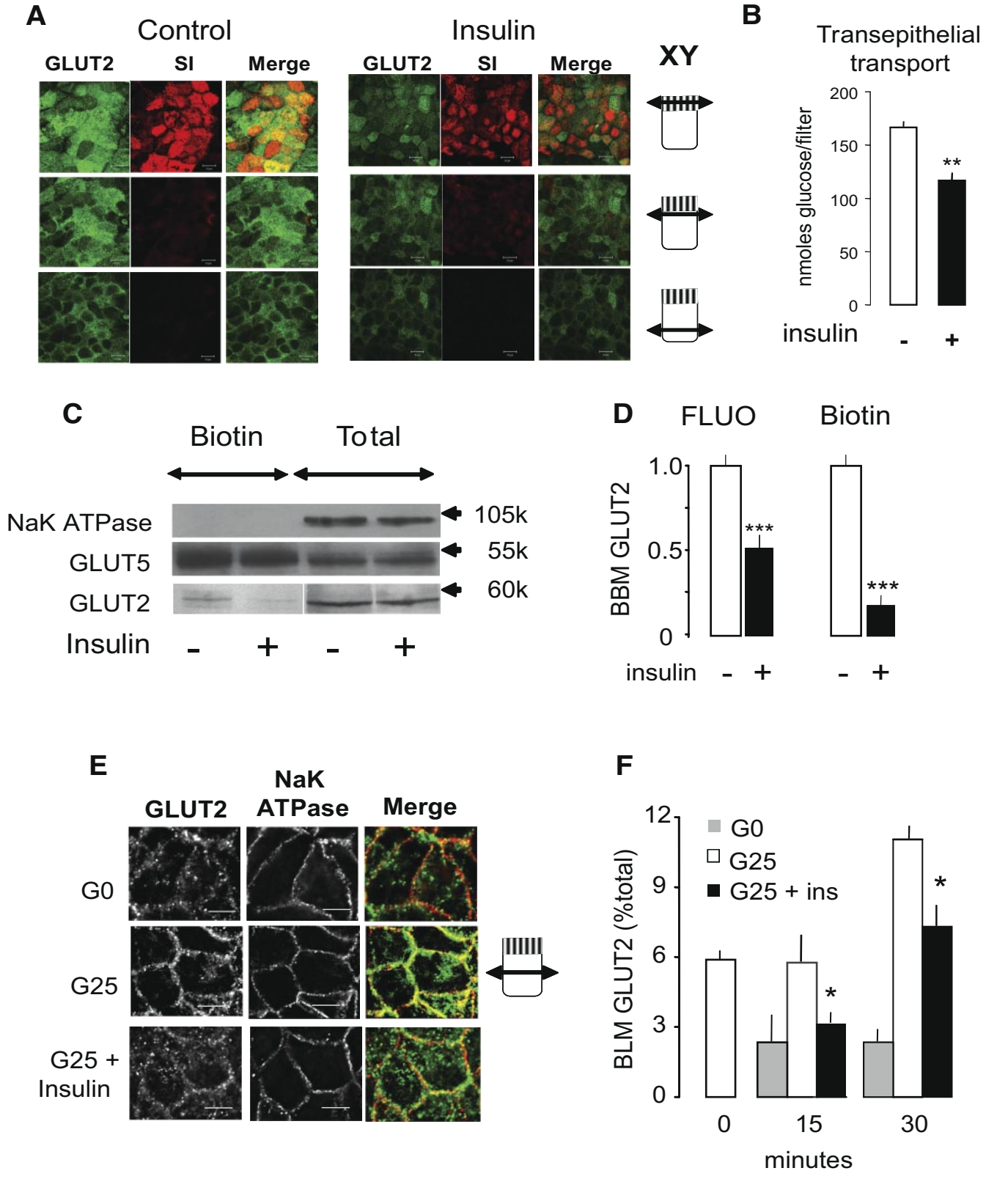

FIG. 1. Impact of insulin on BBM and BLM GLUT2 in Caco-2/TC7 cells. Caco-2/TC7 cells were cultured on a porous support in 25 mmol/l glucose-DMEM for 21 days and exposed to 1 mU/ml insulin for 1 h in serum-free media. *A*: Immunofluorescence study of GLUT2 (CY2, green) and sucrase-isomaltase (CY3, red) membrane colocalization (merge yellow) in control and insulin-treated cells. Confocal images were taken through the BBM plane or just below BBM in a subapical compartment or through nuclei. *B*: Transepithelial transport after 30 min across control and insulin-treated cells was measured using 3-OMG as a tracer. Results in nanomoles ± SE from nine filters are shown. *C*: Surface biotinylation with membrane-impermeant NH-S-S-biotin was performed from the BBM side of cells. Western blots of GLUT2, GLUT5, and NaKATPase in 10% of total protein or biotin proteins purified on Neutravidin columns from 90% total proteins are shown. *D*: Quantification of insulin effects by colocalization of GLUT2 and sucrase-isomaltase over total sucrase-isomaltase–positive cells (Fluo) counted from four independent cultures with 10 fields and 200 control and 200 insulin-treated cells. Scan density analyses of biotin-GLUT2 in insulin-treated cells (Biotin) were quantified in eight monolayers from four experiments and expressed relative to biotin-GLUT2 in parallel control cells. *E* and *F*: Deconvoluted images taken

RESEARCH DESIGN AND METHODS

Cell culture. Caco-2/TC7 on cells filters (3 μm HD; BD Biosciences, Pont de Claix, France) were grown in Dulbecco's modified Eagle's medium (DMEM; Gibco, Paisley, U.K.) supplemented with 25 mmol/l glucose and 10% decomplemented FCS (AbCys, Paris, France) (15). Insulin stimulation (1 mU/ml in basolateral compartment, 1 h, 37°C) was performed in serum-free media. Differentiated cells were washed with ice-cold PBS/Ca^{2+}/Mg^{2+} buffer before processing.

Fluorescence microscopy, image acquisition, and treatment. Caco-2/TC7 cells were fixed with 4% paraformaldehyde (wt/vol) at 4°C, and antibody labeling was made on permeabilized cells with 1% Triton X-100. Antibodies were added for 1 h, and extensive washing with PBS/glycine buffer was performed between steps. Secondary antibodies were labeled with cyanin. Images were taken using a confocal microscope (LSM 510; Zeiss) and Leica DMRXA microscope with CCD camera (5MHz Micromax 1300Y; Roper Instruments) with the Metamorph software (Universal Imaging) to deconvolute Z-series. Colocalizations were analyzed with ImageJ1.37 software (http://rsb.info.nih.gov).

Cell surface biotinylation. Cells were labeled from the BLM or BBM side with 1 mg/ml membrane-impermeant sulfo-NHSS-biotin and biotinylated proteins purified on NeutrAvidin gel columns (Pierce, Rockford, IL) as described previously (11).

Insulin signaling pathway. Total AKT and phospho-AKT contents were evaluated on frozen cells. Western blots on cleared lysates (20 mmol/l Tris, 150 mmol/l NaCl, 5 mmol/l EDTA, 1% [vol/vol] Triton X-100, and 0.5% deoxycholate) were revealed with specific AKT and Ser^{473}P-AKT antibodies (Cell Signaling Technologies).

Animals. C57bl/6J mice were fed with isocaloric 65% glucose-, fructose-, or protein-rich diets (6) or 72% fat, low-sugar (18) or standard chow (M25; Safe, Augy, France). Body weights of standard chow– and fructose-fed age-matched mice after 30 days (23.5 ± 0.5 vs. 23.10 ± 0.4 g; $n = 24$) and age-matched mice fed standard chow and high-fat diets after 4 months (27.4 ± 0.3 vs. 24.6 ± 0.4 g; $n = 20$) were similar. Gavages were performed after an 18-h fast using saline or 4 mg/g body wt glucose or fructose solutions. Intraperitoneal injections of saline (sham) or 1 mU/kg insulin (Actrapid; Novo Nordisk) were performed 20 min before gavage. Tail blood glucose (Accu-check; Roche Diagnostic) and plasma insulin (EIA; Linco Research, St. Charles, MO) were measured. The hyperinsulinemic-euglycemic clamp experiments were performed in conscious mice after a 5-h fast (19). Insulin perfusions in the jugular vein were at 0.6 $mU \cdot kg^{-1} \cdot h^{-1}$ and 15 g/dl glucose at variable rate to maintain euglycemia (fructose diet: clamp 122 ± 17 mg/dl [$n = 9$], sham 135 ± 10 mg/dl [$n = 9$]; high-fat diet: clamp 148 ± 37 [$n = 4$], sham 152 ± 15 [$n = 4$]). Glucose infusion rates (GIRs) were calculated at the end of a 40-min clamp.

Membrane preparations. Fresh jejunal mucosa scrapings were processed for membrane preparations. Membrane fractionations in iodixanol (Optiprep Abscys) gradients performed as described previously (20) with 6 mg protein (BCA protein kit; Pierce) were laid on top of a 7.5–30% gradient, and step fractions (500 μl) were collected for density quantifications and Western blot analysis. BBM were purified using the $MgCl_2$/EGTA precipitation method (21).

Western blotting. Western blots were performed as described previously (6). Primary antibodies against rGLUT5, hGLUT5-Cterm (22), sucrase-isomaltase (23), NaKATPase-α1 (Abcam, Cambridge, U.K.), insulin receptor-β1 (Santa Cruz Biotechnology, Santa Cruz, CA), and peptide transporter-1 (PepT1) were used. For GLUT2 labels, rhGLUT2 (extracellular TM1-TM2 loop) (6), hmGLUT2 (Santa Cruz Biotechnology), and hGLUT2-Nter peptide gave similar results.

Sugar transport assays. The transepithelial transfer of [^{3}H]-3-*O*-methyl-glucose (3-OMG) in 25 mmol/l glucose-DMEM was measured in control and insulin-treated Caco-2/TC7 cells. The radioactivity was added at the BBM side of cells and 50-μl triplicate BLM medium samples were counted after 30 min. The results are picomoles ± SE from nine filters. Fructose uptake in jejunal tissue rings was measured as described previously (6). Uptakes are in nanomoles per milligram protein per second.

Statistics. Results are given as means ± SEM (n), and ANOVA tests were performed.

RESULTS

BBM GLUT2 is decreased by insulin in Caco-2-TC7 cells. The effects of insulin on enterocytes were studied in Caco-2/TC7 cells (15,24), which enabled a separation between the effects of insulin and glucose in vitro. Differentiated Caco-2/TC7 cells segregate sucrase-isomaltase in BBM and NaKATPase in BLM (Supplemental Fig. 1*A*, available in an online appendix at http://dx.doi.org/10.2337/db07-0928).

The β1-insulin receptor was found in BBM and BLM and in intracellular stores (XZ sections). In this experimental setting, glucose was added to the apical side and insulin to the basolateral side of the cells to mimic in vivo sugar absorption. Culture media were supplemented with 10% FCS containing insulin that could induce internalization of the insulin receptor. Glucose concentrations had not changed significantly at harvest (not shown). Insulin receptors were functional, as shown by AKT phosphorylation kinetics (Supplemental Fig. 1*B*).

Confocal microscopy analysis of the colocalization of GLUT2 with sucrase-isomaltase (Fig. 1*A*) indicated that GLUT2 was associated with BBM. GLUT2 was also abundant in subapical compartments where sucrase-isomaltase was undetectable. The quantification of GLUT2 and sucrase-isomaltase colocalization (Fig. 1*A*, Merge, line 1) indicated that 1 mU/ml insulin reduced BBM GLUT2 by 60% (Fig. 1*D*, Fluo).

To distinguish GLUT2 in intracellular membranes from BBM GLUT2, we performed surface biotinylation of proteins with impermeant NHSS-biotin. When biotin was added to the BBM side of cells, Western blotting of biotinylated proteins revealed GLUT5 and GLUT2 in BBM (Fig. 1*C*). NaKATPase could be biotinylated from the BLM (data not shown) but not from the BBM side of cells (Fig. 1*C*), indicating integrity of intercellular tight junctions. After exposure to insulin for 1 h, GLUT5, GLUT2, and NaKATPase levels in total membranes were unchanged (Fig. 1*C*), but BBM GLUT2 levels decreased by 80% (Fig. 1*D*, Biotin), whereas GLUT5 remained unchanged.

A precise deconvoluted image of a single microscopy section at mid-height of enterocytes shows association of GLUT2 with BLM identified by NaKATPase labeling (Fig. 1*E*). The addition of 25 mmol/l glucose increased BLM GLUT2 twofold after 15 min and fourfold after 30 min compared with sugar-deprived cells (Fig. 1*F*). BLM GLUT2 at 30 min contained 12% of total GLUT2 in whole cell. Insulin treatment decreased BLM GLUT2 by 45 and 34% after 15 and 30 min, respectively ($P < 0.05$) (Fig. 1*F*).

To determine the functional consequences of insulin action, we measured the transfer of the nonmetabolizable glucose analog 3-OMG from the apical to the basolateral compartment. The results revealed a 30% ($P < 0.01$) inhibition after a 30-min insulin treatment (Fig. 1*B*), which reflected the inhibition of GLUT2-mediated transport in Caco-2/TC7 cells. Thus insulin decreases BBM and BLM GLUT2 levels in enterocytes and limits the transepithelial transport of sugars by a specific internalization of GLUT2 from plasma membranes.

High-fructose or high-fat feeding on intestinal GLUT2 expression and glucose homeostasis in mice in vivo. Mice fed a fructose-rich diet had a twofold (2.25 ± 0.9; $n = 14$) higher expression of GLUT2 in the jejunum compared with chow-fed mice. The maximum increase was attained after 5 days and remained stable thereafter.

at a single plane are shown. *E*: BLM GLUT2 (CY2) and NaKATPase (CY3) in one representative experiment of three, showing cells cultured in glucose-free medium (G0), in glucose (G25), or in glucose with 1 mU/l insulin. *F*: The colocalization of GLUT2 with NaKATPase was quantified in all the planes imaging the whole cell and expressed as percent of total GLUT2 in glucose- and/or insulin-treated cells. ***$P < 0.001$; **$P < 0.01$; *$P < 0.05$. (Please see http://dx.doi.org/10.2337/db07-0928 for a high-quality digital representation of this figure.)

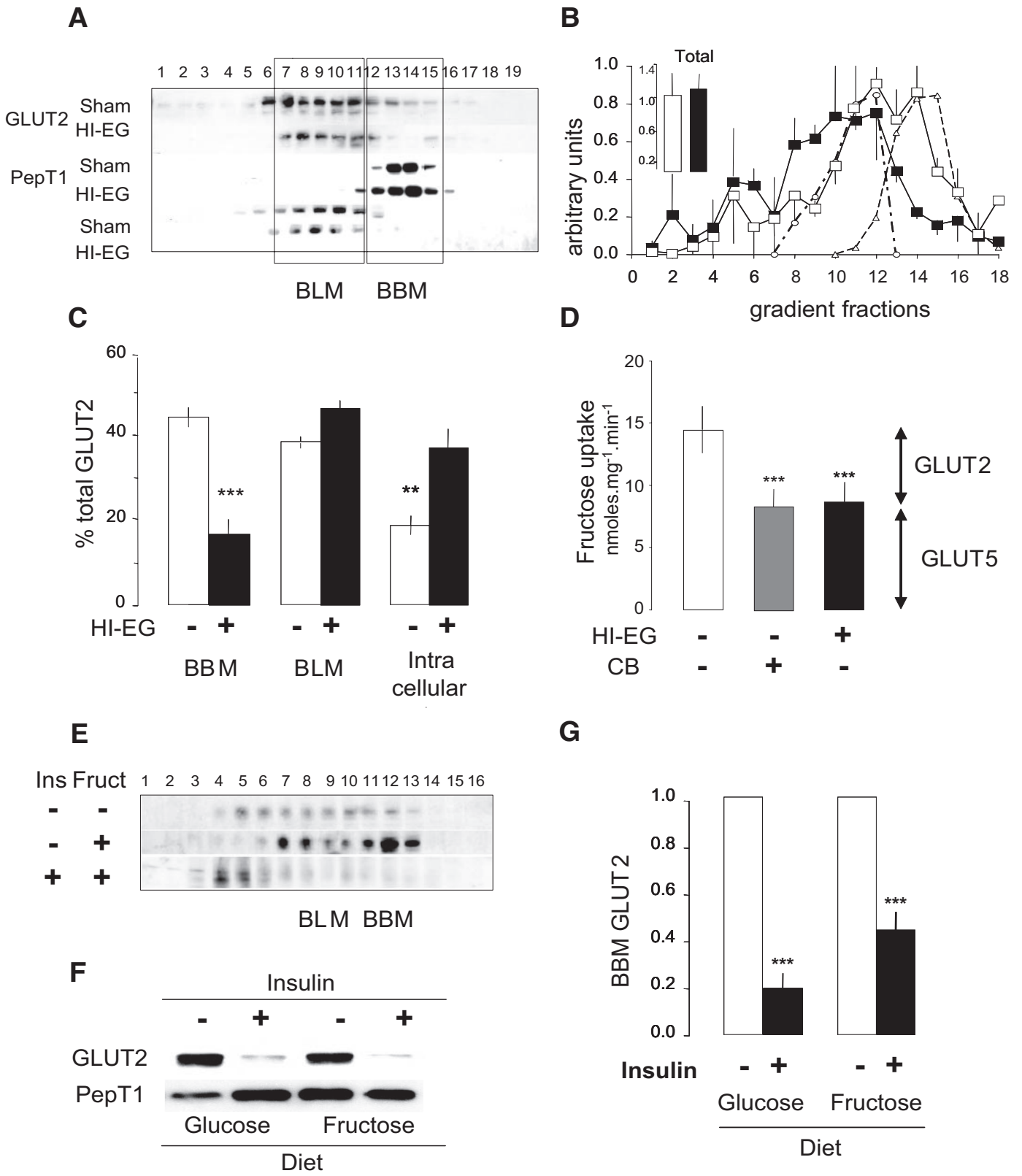

FIG. 2. GLUT2 membrane trafficking in insulin-sensitive mice. *A–C*: Hyperinsulinemic-euglycemic clamp experiment in mice. *A*: Western blot of GLUT2, PepT1, and NaKATPase abundance in fractions of iodixanol density-gradient of total membranes prepared from a single intestine in either sham or hyperinsulinemic-euglycemic clamp conditions. Hyperinsulinemic-euglycemic clamp experiments were performed after a 5-h fast in mice fed a high-fructose diet for 15 days. The intestines of sham and hyperinsulinemic-euglycemic mice were taken at the end of a 2-h clamp. Gradient fractions are sorted from left to right by increasing densities ranging from 1.06 to 1.16 g/ml. *B*: Quantification of NaKATPase (○), PepT1 (△), and GLUT2 in fractions from four paired sham (□) and hyperinsulinemic-euglycemic (■) mice. Scan densities are shown as ratios of protein levels in a fraction to its maximum level in the gradient (arbitrary units ± SE). *Inset*: GLUT2 in the total membranes loaded on gradients (sham, □; hyperinsulinemic-euglycemic, ■). *C*: GLUT2 membrane distribution calculated from *B* in BBM (sum in fractions containing PepT1), BLM (sum in fractions containing NaKATPase), and nonplasma membranes (intracellular membranes; all other fractions). *D*: Fructose uptake (10 mmol/l for 2 min at 37°C) in jejunal everted rings from sham (□; $n = 3$) and hyperinsulinemic-euglycemic (■; $n = 3$) and sham after 100 μmol/l

On the contrary, mice fed a high-fat diet expressed basal levels of GLUT2 (1.04 ± 0.3; $n = 7$) like chow-fed mice.

The consumption of fructose-rich and high-fat diets perturbed mice glucose homeostasis (Supplemental Table 1, online appendix). Glucose intolerance (ΔG) was found as soon as 5 days after the beginning of the fructose diet and after 3 months of fat feeding (not shown). Increased ΔG-to-ΔI ratios indicated that mice became insulin-resistant and fasting blood glucose levels were slightly increased.

To investigate insulin action in the intestine, we performed hyperinsulinemic-euglycemic clamps in conscious mice. Moderate hyperinsulinemia (2.36 ± 0.34 vs. 0.49 ± 0.05 ng/ml; $n = 4$) was obtained. GIRs were similar in chow- and fructose-fed mice for 15 days (67 ± 1 and 65 ± 4 mg · kg^{-1} · min^{-1}; $n = 4$), indicating similar insulin sensitivity. However, GIRs were decreased at day 30 in fructose-fed mice, indicating that they were insulin resistant (36 ± 6 mg · kg^{-1} · min^{-1}; $n = 6$). The GIR of mice fed a high-fat diet for 4 months was reduced even more (7 ± 4 mg · kg^{-1} · min^{-1}; $n = 6$), indicating very high insulin resistance. We were then able to study insulin effects on GLUT2 trafficking by comparing sensitive and resistant mice.

Insulin action on the membrane distribution of GLUT2 in insulin-sensitive mice. Enterocyte membranes were separated according to densities (1.057–1.150 g/l) in iodixanol gradients (20). GLUT2 was found in BBM fractions containing the PepT1 marker and in BLM containing the NaKATPase marker (Fig. 2*A* and *B*). Intracellular (non-BBM, non-BLM) membranes also contained GLUT2. These results confirmed the presence of GLUT2 in BBM and intracellular GLUT2 stores in vivo.

Insulin lowered GLUT2 by 60% in PepT1 fractions, indicating removal from BBM (Fig. 2*B* and *C*) in absence of major protein degradation because total GLUT2 levels in sham and hyperinsulinemic-euglycemic clamp conditions were unchanged (Fig. 2*B*, *inset*). Accordingly, GLUT2 increased in intracellular membranes (Fig. 2*C*). Thus, insulin promoted GLUT2 internalization from BBM to intracellular membrane stores.

The functional significance of the insulin-dependent internalization of BBM GLUT2 with respect to sugar absorption was measured in everted jejunal rings of sham and hyperinsulinemic-euglycemic mice (Fig. 2*D*). Insulin reduced fructose uptake by 40% ($P < 0.001$), indicating that sugar transport correlated to BBM transporter abundance. We used cytochalasin B to determine the contributions of GLUT2 and GLUT5 (insensitive to cytochalasin B) to fructose uptake. Fructose uptakes were identical in hyperinsulinemic-euglycemic and sham mice exposed to cytochalasin B, thus confirming that insulin did not change localization and activity of GLUT5. Insulin specifically decreases GLUT2-dependent fructose transport.

Impairment of GLUT2 trafficking by insulin injection before a sugar bolus. The effect of insulin in hyperinsulinemic-euglycemic mice reduced GLUT2-dependent fructose uptake in conditions of fast. During a sugar meal, luminal sugars are high, triggering GLUT2 translocation to the BBM, and then blood glucose and plasma insulin rise. To document the impact of luminal sugar and insulin on the distribution of GLUT2 in enterocyte membranes, we force-fed insulin-sensitive mice with fructose and elicited GLUT2 trafficking into BBM (Fig. 2*E–G*).

Intraperitoneal insulin injections performed 20 min before the fructose test meal produced a threefold elevation of plasma insulin (range 1.2–1.7 ng/ml) to a level similar to that produced during hyperinsulinemic-euglycemic clamp. The recruitment of GLUT2 into BBM in response to luminal fructose was abolished by insulin injection, and the distribution of GLUT2 was similar to that in enterocytes of fasted mice (Fig. 2*E*). Interestingly, insulin effects tended to be weaker in purified BBM from mice fed 5 days with the fructose-rich compared with the glucose-rich diet (Fig. 2*G*). Prior insulin treatment counteracted the insertion of GLUT2 into BBM induced by luminal dietary sugar (Fig. 2*E*).

GLUT2 membrane distribution and trafficking in insulin-resistant mice. The membrane distribution of GLUT2 in insulin-resistant mice obtained by prolonged fructose (Fig. 3*A–C*) or fat feeding (Fig. 3*D–F*) was markedly perturbed. High levels of GLUT2 were found in BBM-PepT1 fractions (Fig. 3*A* and *D*), which represented 40% of total GLUT2 in the enterocyte membranes of mice fed fructose-rich diet for 30 days (Fig. 3*C*). This proportion increased to 80% in high-fat conditions (Fig. 3*E*). BLM GLUT2 levels were 10% (high-fructose; Fig. 3*C*) and 20% (high-fat; Fig. 3*F*) of total GLUT2 compared with 40% in insulin-sensitive mice (Fig. 2*C*). The functional impact of this redistribution of GLUT2 was revealed by the twofold increase in the initial slope (0–15 min) of blood glucose after an oral glucose tolerance test in resistant mice (high fat 0.30 ± 0.02 mg · dl^{-1} · min^{-1}; high fructose 0.28 ± 0.01 mg · dl^{-1} · min^{-1}; $n = 8$) compared with sensitive mice (0.13 ± 0.01 mg · dl^{-1} · min^{-1}; $n = 8$; $P < 0.001$). Thus in insulin-resistant states, BBM GLUT2 was high and increased blood glucose entry.

In insulin-resistant mice, BBM localizations were unaffected by insulin in hyperinsulinemic-euglycemic clamp conditions. BLM GLUT2 remained <20% of total GLUT2 (Fig. 3*C* and *F*). In addition, BBM GLUT2 levels were correlated with GIR. Insulin-resistant mice exhibited a loss of control by insulin of GLUT2 membrane trafficking, leading to a permanent localization of GLUT2 in enterocyte BBM, a pathological consequence of long-term fructose or fat feeding.

DISCUSSION

We had previously reported the rapid and transient recruitment of GLUT2 into enterocyte BBM after a bolus of simple sugars, generating a threefold enhancement of uptake (6). The present study demonstrates and quantifies in vitro and in vivo the inhibition by insulin of intestinal sugar uptake, as a result of the internalization of GLUT2 from plasma membranes back into intracellular pools.

cytochalasin B preincubation for 10 min (▨; $n = 3$). Uptakes were measured in individual mice intestines (12 rings per mouse). *E–G*: Effect of an insulin injection before a fructose test meal. Mice were fed a fructose diet for 5 days and fasted overnight. Mice were then injected intraperitoneally either PBS or insulin (1 mU/kg) 20 min before a fructose (90 mg/kg) test meal. Intestines were taken 30 min after the test meal. *E*: Representative Western blot (12 mice in four experiments) of the distribution of GLUT2 in iodixanol fractions. Fractions containing BLM (NaKATPase) and BBM (PepT1) have been boxed for clarity. *F*: Comparison of the effect of a 5-day glucose-rich or fructose-rich diet on BBM GLUT2 levels in the response to an insulin injection prior a fructose test meal (protocol similar to *E*). Representative Western blot of purified jejunal BBM using the Mg^{2+}/EGTA precipitation method. *G*: Scan density quantification (means ± SE; $n = 6$) of BBM GLUT2 in conditions of PBS (□) or 1 mU/kg insulin (■). ***$P < 0.001$; **$P < 0.01$.

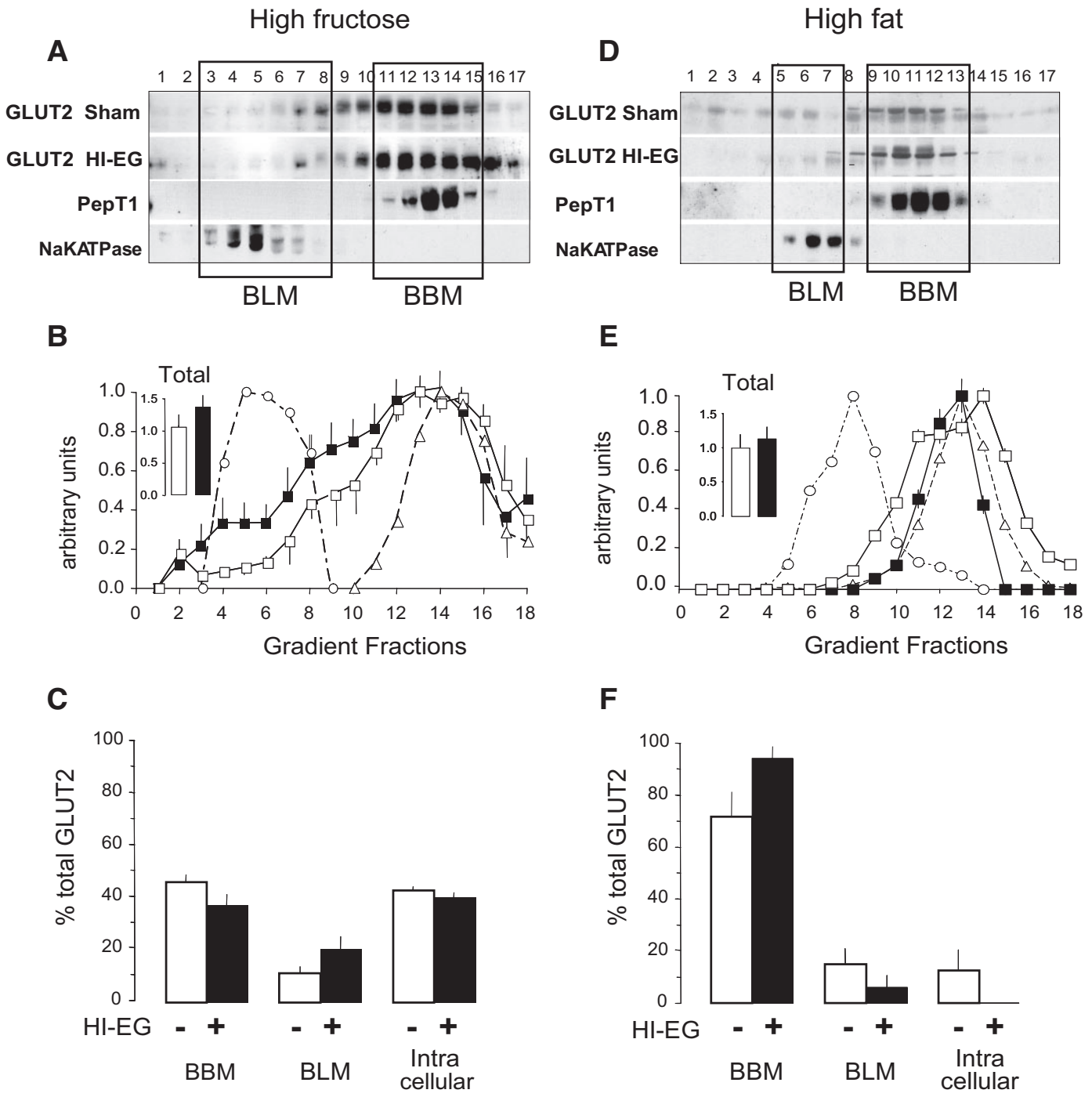

FIG. 3. Insulin resistance remodels the distribution of GLUT2 in enterocyte membranes. Insulin resistance was induced in mice by feeding a fructose-rich diet for 30 days (*A–C*) or a high-fat diet for 4 months (*D–F*), and intestines were processed as described in Fig. 2. *A* and *D*: Western blot (out of 4) of GLUT2, PepT1, and NaKATPase in sham and hyperinsulinemic-euglycemic clamp in mice. *B* and *E*: Average values from four mice of GLUT2, NaKATPase, and PepT1 protein abundance in gradient fractions (same symbols as in Fig. 2*B*). Data are expressed as the ratio of the level of protein in a given fraction to the maximum level of protein in the gradient (arbitrary units ± SE). *Inset*: GLUT2 in the total membranes loaded on gradients (sham, □; hyperinsulinemic-euglycemic, ■). *C* and *F*: GLUT2 membrane distribution calculated from *B* and *E* in BBM (sum in fractions containing PepT1), BLM (sum in fractions containing NaKATPase), and nonplasma membranes (intracellular membranes; all other fractions).

This important physiological process mediated by insulin at the level of enterocytes probably reveals another mechanism by which insulin limits sugar excursion in the blood during a sugar-rich meal. Furthermore, insulin resistance provoked a loss of control by insulin of GLUT2 membrane trafficking, a pathological consequence of the long-term consumption of a fructose-rich or high-fat diet.

Insulin sensitivity and glucose tolerance are important factors in the regulation of intestinal GLUT2 trafficking. In insulin-resistant mice obtained by prolonged fructose-rich or high-fat diets, the distribution of GLUT2 was drastically altered; BBM GLUT2 was permanently high, and insulin was unable to promote GLUT2 internalization and enrichment in intracellular membranes. Insulin resistance resulted in increased intestinal sugar delivery, as reflected by higher initial rise in blood glucose after oral glucose load.

Insulin action is transduced via receptors in enterocyte plasma membranes in vivo (25,26) and in vitro in Caco-2/TC7 cells. The functional significance of BLM insulin receptors is obvious, and we speculate that enterocytes akin to epithelial renal cells undergo a rapid phosphatidylinositol (3,4,5)-trisphosphate diffusion after insulin to trigger trafficking of a BBM protein (27). The role of insulin receptors in the BBM is unclear but it creates an opportunity for oral insulin treatment (28) that might target BBM GLUT2 localization and function. Conflicting results concerning acute insulin treatment report inhibition (14) and activation (29) of SGLT1-dependent intestinal sugar absorption ex vivo. In the present work, we describe an insulin action on the high capacity GLUT2 component of fructose transport that leads to a 50% inhibition of total transport, down to GLUT5 basal transport levels. We speculate that this regulation applies to intestinal glucose absorption. In insulin-resistant animals, a permanent BBM GLUT2 might create glucose efflux from enterocytes into the lumen. This is unlikely because permanent SGLT1 recapture would operate. These results highlight the complexity of the regulation of intestinal sugar absorption by insulin to modulate but not block intestinal sugar absorption.

In adipocytes and muscle cells, insulin provokes a massive translocation of GLUT4 to the plasma membrane (rev. in 12,30). In sharp contrast, insulin internalizes BBM GLUT2 into intracellular pools. Insulin, by regulating GLUT2 and GLUT4 traffic in opposite direction, controls glucose homeostasis and limits glucose excursion in the course of digestion by increasing peripheral GLUT4-dependent glucose uptake and slowing down intestinal GLUT2-dependent sugar delivery. We therefore propose that the small intestine constitutes an early checkpoint to limit postprandial glucose excursion. We also anticipate that insulin treatment will remove GLUT2 from its permanent BBM localization in type I diabetic patients that are insulin sensitive.

Modern westernized diets and eating habits have changed, increasing the amounts of dietary fructose and fat, which are probably a nutritional basis for the obesity and type 2 diabetes pandemics (31). Intestinal adaptation to these diets may be an early event to the onset of metabolic disorders due to the rapid increase in sugar transport capacities and the alteration of insulin action in enterocytes. With time, insulin resistance and metabolic disorders (32) might be worsen by uncontrolled sugar absorption in a small intestine that is no longer responsive to attenuation by insulin. A vicious circle thus develops that equips the intestine for high transport of dietary sugar in organisms already suffering from excessive blood glucose levels. Strategies to ameliorate insulin action on intestinal function therefore constitute another target for therapeutic intervention and control of postprandial glycemia.

ACKNOWLEDGMENTS

V.T. has received an MRT PhD fellowship. M.L.G. has received a Benjamin Delessert prize. E.S. has received an MRT PhD fellowship. A.G.B. has received a grant from FPI Spanish Ministerio de Educacion y Ciencia (BES-2004-4685). This work has received support from Institut National de la Santé et de la Recherche Médicale, University Paris 6, Action Thematique Concertée (ATC) Nutrition (ASEO22129DSA), ALFEDIAM/Merk-Lipha grants.

We thank E. Petridi and V. Ondet for their contribution and C. Lasne and E. Dussaulx for technical assistance. We are grateful to J. Chambaz for support, to G.W. Gould (Glasgow, U.K.) for antibodies, and to G.L. Kellett (York, U.K.) for antibodies and for fruitful discussions.

REFERENCES

1. Wright EM, Martin MG, Turk E: Intestinal absorption in health and disease: sugars. *Best Pract Res Clin Gastroenterol* 17:943–956, 2003
2. Thorens B: Molecular and cellular physiology of GLUT-2, a high-Km facilitated diffusion glucose transporter. *Int Rev Cytol* 137:209–238, 1992
3. Cheeseman CI: GLUT2 is the transporter for fructose across the rat intestinal basolateral membrane. *Gastroenterology* 105:1050–1056, 1993
4. Helliwell PA, Richardson M, Affleck J, Kellett GL: Regulation of GLUT5, GLUT2 and intestinal brush-border fructose absorption by the extracellular signal-regulated kinase, p38 mitogen-activated kinase and phosphatidylinositol 3-kinase intracellular signalling pathways: implications for adaptation to diabetes. *Biochem J* 350:163–169, 2000
5. Kellett GL, Brot-Laroche E: Apical GLUT2: a major pathway of intestinal sugar absorption. *Diabetes* 54:3056–3062, 2005
6. Gouyon F, Caillaud L, Carriere V, Klein C, Dalet V, Citadelle D, Kellett GL, Thorens B, Leturque A, Brot-Laroche E: Simple-sugar meals target GLUT2 at enterocyte apical membranes to improve sugar absorption: a study in GLUT2-null mice. *J Physiol* 552:823–832, 2003
7. Walker J, Jijon HB, Diaz H, Salehi P, Churchill T, Madsen KL: 5-Aminoimidazole-4-carboxamide riboside (AICAR) enhances GLUT2-dependent jejunal glucose transport: a possible role for AMPK. *Biochem J* 385:485–491, 2005
8. Madsen KL, Ariano D, Fedorak RN: Insulin downregulates diabetic-enhanced intestinal glucose transport rapidly in ileum and slowly in jejunum. *Can J Physiol Pharmacol* 74:1294–1301, 1996
9. Habold C, Foltzer-Jourdainne C, Le Maho Y, Lignot JH, Oudart H: Intestinal gluconeogenesis and glucose transport according to body fuel availability in rats. *J Physiol* 566:575–586, 2005
10. Baba R, Yamami M, Sakuma Y, Fujita M, Fujimoto S: Relationship between glucose transporter and changes in the absorptive system in small intestinal absorptive cells during the weaning process. *Med Mol Morphol* 38:47–53, 2005
11. Au A, Gupta A, Schembri P, Cheeseman CI: Rapid insertion of GLUT2 into the rat jejunal brush-border membrane promoted by glucagon-like peptide 2. *Biochem J* 367:247–254, 2002
12. Huang S, Czech MP: The GLUT4 glucose transporter. *Cell Metab* 5:237–252, 2007
13. Corpe CP, Basaleh MM, Affleck J, Gould G, Jess TJ, Kellett GL: The regulation of GLUT5 and GLUT2 activity in the adaptation of intestinal brush-border fructose transport in diabetes. *Pflugers Arch* 432:192–201, 1996
14. Pennington AM, Corpe CP, Kellett GL: Rapid regulation of rat jejunal glucose transport by insulin in a luminally and vascularly perfused preparation. *J Physiol* 478:187–193, 1994
15. Mahraoui L, Rodolosse A, Barbat A, Dussaulx E, Zweibaum A, Rousset M, Brot-Laroche E: Presence and differential expression of SGLT1, GLUT1, GLUT2, GLUT3 and GLUT5 hexose-transporter mRNAs in Caco-2 cell clones in relation to cell growth and glucose consumption. *Biochem J* 298:629–633, 1994
16. Havel PJ: Dietary fructose: implications for dysregulation of energy homeostasis and lipid/carbohydrate metabolism. *Nutr Rev* 63:133–157, 2005
17. Jurgens H, Haass W, Castaneda TR, Schurmann A, Koebnick C, Dombrowski F, Otto B, Nawrocki AR, Scherer PE, Spranger J, Ristow M, Joost HG, Havel PJ, Tschop MH: Consuming fructose-sweetened beverages increases body adiposity in mice. *Obes Res* 13:1146–1156, 2005
18. Burcelin R, Dolci W, Thorens B: Long-lasting antidiabetic effect of a dipeptidyl peptidase IV-resistant analog of glucagon-like peptide-1. *Metabolism* 48:252–258, 1999
19. Ayala JE, Bracy DP, McGuinness OP, Wasserman DH: Considerations in the design of hyperinsulinemic-euglycemic clamps in the conscious mouse. *Diabetes* 55:390–397, 2006
20. Li X, Zhang H, Cheong A, Leu S, Chen Y, Elowsky CG, Donowitz M: Carbachol regulation of rabbit ileal brush border Na+-H+ exchanger 3 (NHE3) occurs through changes in NHE3 trafficking and complex formation and is Src dependent. *J Physiol* 556:791–804, 2004
21. Brot-Laroche E, Dao MT, Alcalde AI, Delhomme B, Triadou N, Alvarado F: Independent modulation by food supply of two distinct sodium-activated D-glucose transport systems in the guinea pig jejunal brush-border membrane. *Proc Natl Acad Sci U S A* 85:6370–6373, 1988
22. Mahraoui L, Rousset M, Dussaulx E, Darmoul D, Zweibaum A, Brot-

Laroche E: Expression and localization of GLUT-5 in Caco-2 cells, human small intestine, and colon. *Am J Physiol* 263:G312–G318, 1992
23. Zweibaum A, Hauri HP, Sterchi E, Chantret I, Haffen K, Bamat J, Sordat B: Immunohistological evidence, obtained with monoclonal antibodies, of small intestinal brush border hydrolases in human colon cancers and foetal colons. *Int J Cancer* 34:591–598, 1984
24. Delie F, Rubas W: A human colonic cell line sharing similarities with enterocytes as a model to examine oral absorption: advantages and limitations of the Caco-2 model. *Crit Rev Ther Drug Carrier Syst* 14:221–286, 1997
25. Bergeron JJ, Rachubinski R, Searle N, Borts D, Sikstrom R, Posner BI: Polypeptide hormone receptors in vivo: demonstration of insulin binding to adrenal gland and gastrointestinal epithelium by quantitative radioautography. *J Histochem Cytochem* 28:824–835, 1980
26. Buts JP, De Keyser N, Sokal EM, Marandi S: Oral insulin is biologically active on rat immature enterocytes. *J Pediatr Gastroenterol Nutr* 25:230–232, 1997
27. Blazer-Yost BL, Vahle JC, Byars JM, Bacallao RL: Real-time three-dimensional imaging of lipid signal transduction: apical membrane insertion of epithelial Na(+) channels. *Am J Physiol Cell Physiol* 287:C1569–C1576, 2004
28. Damge C, Maincent P, Ubrich N: Oral delivery of insulin associated to polymeric nanoparticles in diabetic rats. *J Control Release* 117:163–170, 2007
29. Stumpel F, Kucera T, Gardemann A, Jungermann K: Acute increase by portal insulin in intestinal glucose absorption via hepatoenteral nerves in the rat. *Gastroenterology* 110:1863–1869, 1996
30. He A, Liu X, Liu L, Chang Y, Fang F: How many signals impinge on GLUT4 activation by insulin? *Cell Signal* 19:1–7, 2007
31. Basciano H, Federico L, Adeli K: Fructose, insulin resistance, and metabolic dyslipidemia. *Nutr Metab* (*Lond*) 2:5, 2005
32. Le KA, Tappy L: Metabolic effects of fructose. *Curr Opin Clin Nutr Metab Care* 9:469–475, 2006